



Heterogeneous & Homogeneous & Bio- & Nano-

# CHEM **CAT** CHEM

---

## CATALYSIS

### Accepted Article

**Title:** Enhanced catalytic properties of carbons supported zirconia (Zr) and sulfated zirconia (SZr) in the green synthesis of benzodiazepines

**Authors:** Marina Godino-Ojer, Leticia Milla-Diez, Ines Matos, Carlos J. Durán-Valle, Maria Bernardo, Isabel M. Fonseca, and Elena Perez-Mayoral

This manuscript has been accepted after peer review and appears as an Accepted Article online prior to editing, proofing, and formal publication of the final Version of Record (VoR). This work is currently citable by using the Digital Object Identifier (DOI) given below. The VoR will be published online in Early View as soon as possible and may be different to this Accepted Article as a result of editing. Readers should obtain the VoR from the journal website shown below when it is published to ensure accuracy of information. The authors are responsible for the content of this Accepted Article.

**To be cited as:** *ChemCatChem* 10.1002/cctc.201801274

**Link to VoR:** <http://dx.doi.org/10.1002/cctc.201801274>

WILEY-VCH

[www.chemcatchem.org](http://www.chemcatchem.org)



# Enhanced catalytic properties of carbons supported zirconia (Zr) and sulfated zirconia (SZr) in the green synthesis of benzodiazepines

M. Godino-Ojer,<sup>[a]</sup> L. Milla-Diez,<sup>[a]</sup> I. Matos,<sup>[b]</sup> C. J. Durán-Valle,<sup>[c]</sup> M. Bernardo,<sup>[b]</sup> I. M. Fonseca<sup>\*,[b]</sup> and E. Pérez Mayoral<sup>\*,[a]</sup>

**Abstract:** This work reports for the first time a new series of promising porous catalytic carbon materials, functionalized with Lewis and Brønsted acid sites useful in the green synthesis of 2,3-dihydro-1*H*-1,5-benzodiazepine - nitrogen heterocyclic compounds. Benzodiazepines and derivatives are fine chemicals exhibiting interesting therapeutic properties. Carbon materials have been barely investigated in the synthesis of this type of compounds.

Two commercial carbon materials were selected exhibiting different textural properties: i) Norit RX3 (N) as microporous sample and ii) mesoporous xerogel (X), both used as supports of ZrO<sub>2</sub> (Zr) and ZrO<sub>2</sub>/SO<sub>4</sub><sup>2-</sup> (SZr).

The supported SZr led to higher conversion values and selectivities to the target benzodiazepine. Both chemical and textural properties influenced significantly the catalytic performance.

Particularly relevant are the results concerning the non-sulfated samples, NZr and XZr, that were able to catalyze the reaction leading to the target benzodiazepine with high selectivity (up to 80%; 2h). These results indicated an important role of the carbon own surface functional groups, avoiding the use of H<sub>2</sub>SO<sub>4</sub>. Even very low amounts of SZr supported on carbon reveal high activity and selectivity. Therefore, the carbon materials herein reported can be considered as efficient and sustainable alternative bifunctional catalysts for the benzodiazepine synthesis.

## Introduction

Carbons are considered low cost materials able to act as catalysts or even as supports of active sites meeting the specifications for much more green and sustainable chemical synthesis.<sup>[1]</sup> Carbon-based materials show unique characteristics, among them high thermal and chemical stability,

in acid or basic media, low corrosion capability, hydrophobic character, easy recovery from the reaction mixture and also their biocompatibility, which make them excellent candidates as supports of choice for catalytic purposes. Interestingly, the chemical surface and textural properties of carbon materials are important issues in catalysis, since catalytic activity is depending on the nature and concentration of active sites distributed over the carbon surface as well as the porosity and pore size distribution. The hydrophobicity provided by the carbon materials often comprises the appropriate environment for catalyzing some interesting organic transformations. In this sense, we suspect and recently demonstrated, by using computational methods, the involvement of the carbon surface, through  $\pi$ , $\pi$ -stacking interactions with reagents containing benzene rings, for the synthesis of relevant nitrogen heterocycles via the Friedländer reaction.<sup>[2-4]</sup>

Carbon-supported metal catalysts have been extensively explored in the synthesis of valuable products, some of them exhibiting relevant pharmacological properties.<sup>[5]</sup> Very recently the authors have published for the first time different nanocarbons consisting of carbon aerogels doped with zero-valent transition metals efficiently catalyzing the synthesis of quinolines and related compounds.<sup>[6,7]</sup>

In continuation with ongoing investigations the authors seek to develop new series of bifunctional carbon catalysts incorporating Lewis or/and Brønsted acid sites by modifying the carbon surface with zirconia (Zr) or sulfated zirconia (SZr) able to catalyze the formation of benzodiazepines. SZr and its modified forms are recognized as highly acid catalysts,<sup>[8]</sup> even stronger than traditional H-zeolites,<sup>[9]</sup> frequently explored in the synthesis of a huge number of interesting organic transformations some of them with industrial applications.<sup>[10,11]</sup>

Benzodiazepines are considered as relevant nitrogen heterocyclic systems and their importance is related to diverse pharmacological activities: anti-inflammatory, antiviral, analgesic, anti-microbial, sedative, hypnotic, anti-depressive, anti-tumor, anti-HIV, and also effective on cardiovascular disorders etc.<sup>[12]</sup> Different homogeneous catalysts, mainly consisting of metal transition salts, and also heterogeneous ones, operating under a great variety of reaction conditions have been applied in the synthesis of benzodiazepines from *o*-phenyldiamine and ketones<sup>[13]</sup> Among the most important heterogeneous catalytic systems, it can be cited: zeolites, Al-MCM-41 and Cu(BDC),<sup>[14]</sup> H-MCM-22,<sup>[15]</sup> SiO<sub>2</sub> supporting H<sub>2</sub>SO<sub>4</sub><sup>[16]</sup> and HClO<sub>4</sub>,<sup>[17]</sup> clays<sup>[18-20]</sup> and even SZ.<sup>[21]</sup>

The goal of this paper is, therefore, to perform a comparative study of Zr and SZr catalytic properties with those found for

[a] Ms L. Milla-Díez, Dr. M. Godino-Ojer, Dr. E. Pérez-Mayoral  
Departamento de Química Inorgánica y Química Técnica  
Universidad Nacional de Educación a Distancia, UNED  
Paseo Senda del Rey 9, Facultad de Ciencias  
28040-Madrid (Spain)  
E-mail: eperez@ccia.uned.es

[b] Dr. I. Matos, Dr. M. Bernardo, Dr. I. Fonseca  
LAQV/REQUIMTE, Departamento de Química,  
Faculdade de Ciências e Tecnologia  
Universidade Nova de Lisboa  
2829-516 Caparica (Portugal)

[c] Dr. C. Duran-Valle  
Departamento de Química Orgánica e Inorgánica  
Universidad de Extremadura  
Avda de Elvas, s/n  
E-06006 Badajoz (Spain)

Supporting information for this article is given via a link at the end of the document.

supported carbon with Zr and SZr. It is reasonable to assume that the combination of porous structure of different carbon supports with the highly acidic character of SZr could make these solids interesting catalysts for the green synthesis of 2,3-dihydro-1*H*-1,5-benzodiazepines as an important type of bioactive compounds. Although Zr, particularly its modified form SZr, has been extensively used in industrial reactions, only a few examples of Zr and SZr supported on carbons have been recently reported.

## Results and Discussion

**Synthesis and characterization of the supported Zr catalysts.** Firstly, the Zr and SZr control samples were prepared. Zr was synthesized from  $ZrCl_4$  by treatment with aqueous ammonia solution according to the experimental procedure reported by Scurrill,<sup>[22]</sup> which was subsequently sulfated using  $H_2SO_4$ .<sup>[23]</sup> The synthesis of carbon supported Zr and SZr samples was achieved by adapting this experimental protocol but in the presence of the corresponding carbon material. The carbon supports of our choice were two commercial activated carbons, Norit-RX3(N) and a pure carbon xerogel (X). The obtained carbon supported Zr samples were finally sulfated using two different concentrated  $H_2SO_4$  solutions. Thus, two series of supported carbons were obtained, denoted as NZr and XZr and the corresponding sulfated samples as NZr-S1, NZr-S2 and XZr-S1, XZr-S2 where N and X are Norit-RX3 and xerogel, respectively, Zr is zirconia and S stand for the used  $H_2SO_4$  solutions, concentrated (S1) and diluted (S2).

The surface and bulk properties of the catalysts were studied by  $N_2$  adsorption-desorption, mercury porosimetry, elemental analysis, WDXRF, XPS, thermogravimetry, XRD and SEM-EDS. The textural parameters of the investigated carbon materials changed significantly after modification of the carbon support (Table 1).

All samples derived from Norit-RX3 are mainly microporous samples (pore radius,  $R < 10 \text{ \AA}$ ), barely showing mesopores in the range of 10 to 250  $\text{\AA}$  pore radius. Thus, the  $N_2$  adsorption-desorption isotherms shape are of type I, exhibiting a H4 type hysteresis loop, typical of micro-mesoporous materials. In general, the surface area and pore volume dramatically decrease by the presence of Zr, as expected. However, the pore radius mode calculated by DA method notably increases with the presence of Zr. This feature can be attributed to blockage of the narrowest pores (micropores) by Zr. Thus, the remaining micropores are those with higher width.

Zr and SZr showed a lower  $S_{BET}$ , with similar micro- and macroporous volume. SZr did not show the presence of mesopores. The  $N_2$  adsorption-desorption isotherms of the xerogel type carbons also reveal the mesoporous nature of these materials presenting a type IV isotherm with a type H3 hysteresis loop, typical of materials with mesoporosity. The introduction of Zr strongly influenced the textural parameters with a sharp decrease of surface area and porous volume indicating the possible blockage of pores. The  $E_{ads}$  (Table 1) values, obtained from DR method, for each type of carbon (N or X), followed an inverse trend with microporous radius. Therefore, the narrow pores can lead to adsorption on both sides of the pore, increasing adsorption energy.

Figure 1 depicts the macropore size distribution obtained by Hg porosimetry for Norit-based materials. In general, the supported NZr produces a decrease of mesopore volume,  $V_{meso}$ , but also an increase of macropore volume,  $V_{macro}$  due to the oxide structure. In contrast, treatment of NZr with concentrated  $H_2SO_4$  solution leading to NZr-S1 sample, originated an increase of  $V_{meso}$  and a decrease of  $V_{macro}$ . This circumstance is probably due to the partial solubilization of Zr in the reaction medium. In the case of NZr-S2 sample, it was observed an increase in macroporosity and almost a total disappearance of mesoporosity (Table 1). Regarding the xerogel materials, it can be observed a small decrease on the surface area and on the micro- and mesopore volumes in the supported carbons.

**Table 1.** Textural parameters obtained from  $N_2$  adsorption-desorption isotherms and Hg Porosimetry for carbon materials and Zr-supported carbon materials.

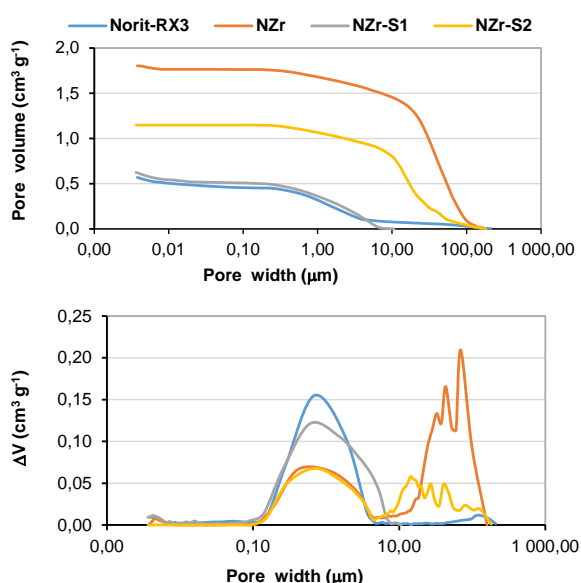
Sample	$S_{BET}^{[a]}$ ( $m^2g^{-1}$ )	$S_{DFT}^{[b]}$ ( $m^2g^{-1}$ )	$V_p^{[b]}$ ( $cm^3g^{-1}$ )	$V_{micro\ DR}^{[c]}$ ( $cm^3g^{-1}$ )	$R^{[c]}$ (nm)	$E_{ads}^{[c]}$ ( $kJmol^{-1}$ )	$V_{micro\ DA}^{[d]}$ ( $cm^3g^{-1}$ )	$R_{moda}^{[d]}$ (nm)	$V_{meso}^{[e]}$ ( $cm^3g^{-1}$ )	$V_{macro}^{[e]}$ ( $cm^3g^{-1}$ )
Zr	348	234	0.33	0.14	0.94	13.85	0.19	0.83	0.15	0.47
SZr	311	232	0.28	0.13	0.86	15.02	0.17	0.79	0.00	0.54
N-RX3	1587	1288	0.73	0.72	1.1	11.96	0.80	0.23	0.10	0.46
NZr	888	707	0.44	0.35	0.71	18.25	0.44	0.71	0.04	1.76
NZr-S1	1247	984	0.56	0.54	0.87	14.83	0.57	0.75	0.11	0.51
NZr-S2	952	737	0.46	0.41	0.89	14.63	0.47	0.73	0.00	1.15
X	595	492	0.47	0.24	1.40	26.04	0.24	1.37	0.24	0.02
XZr-S1	555	460	0.39	0.22	1.41	25.07	0.19	1.36	0.21	0.08
XZr-S2	445	367	0.35	0.17	1.42	24.18	0.18	1.40	0.18	0.06

[a]  $S_{BET}$  = Apparent surface area (BET method). [b]  $S_{DFT}$  = Surface area (Density functional theory, DFT, method),  $V_p$  = pore volume (DFT method), [c]  $V_{micro\ DR}$  = micropore volume (Dubinin-Radushkevich, DR, method),  $R$  = micropore radius (DR method),  $E_{ads}$  =  $N_2$  adsorption energy into micropores (DR method). [d]  $V_{micro\ DA}$  = micropore volume (Dubinin-Astakhov, DA, method),  $R_{moda}$  = micropore radius(DA method) [e]  $V_{meso}$ ,  $V_{macro}$  = meso -macropore volume, by Hg porosimetry

**Table 2.** Composition (expressed on wt%) of the Zr-supported Norit-RX3 carbon materials.

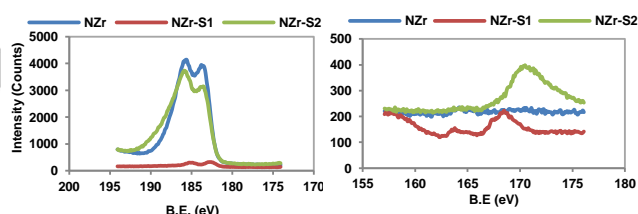
Sample	C 1s <sup>[a]</sup>	O 1s <sup>[a]</sup>	N 1s <sup>[a]</sup>	Si 2p <sup>[a]</sup>	Zr 3d <sup>[a]</sup>	S 2p <sup>[a]</sup>	C <sup>[b]</sup>	H <sup>[b]</sup>	N <sup>[b]</sup>	S <sup>[b]</sup>	O <sup>[b]</sup>	Zr <sup>[c]</sup>	S <sup>[c]</sup>	Zr <sup>[d]</sup>
NZr	46.71	15.47	0.35	1.09	34.90	0.00	81.62	2.54	0.71	0.40	14.73	25.61	0.37	n.d.
NZr-S1	82.68	10.60	0.65	3.28	1.56	0.82	71.97	3.03	0.47	0.84	23.69	1.11	1.04	0.68
NZr-S2	43.12	18.60	0.22	0.00	35.89	2.17	74.03	3.75	0.49	2.27	19.47	22.34	1.00	24.80

Determined by [a] XPS [b] elemental analysis, ash free basis [c]WDXRF [d] ICP-AES; n.d. – not determined

**Figure 1.** Macropore size distribution obtained by Hg porosimetry for Norit-RX3, NZr, NZr-S1 and NZr-S2 samples.

In order to determine the chemical composition, the samples were characterized by elemental analysis, WDXRF and XPS. In the case of samples prepared from Norit-RX3, it can be observed from Table 2 that the S content was notably increased for those submitted to the acid treatment. The sulfur groups are preferentially bound to the Zr surface being higher for the sample NZr-S2, as expected. The increased H% loading from NZr to NZr-S2 may also indicate the small size of graphene sheets especially for the NZr-S2. In the same context, the WDXRF analysis demonstrated that the NZr and NZr-S2 samples showed high Zr loadings. The acid treatment using diluted H<sub>2</sub>SO<sub>4</sub> solution have barely influenced the Zr content – 25.61 and 22.34 expressed in wt. % for NZr and NZr-S2, respectively –. However, the NZr-S1 sample just showed 1.11% of Zr loading. The same behavior was observed for the xerogel carbons. Even though the amount of Zr in samples XZr (10.2 wt%) and XZr-S2 (7.6 wt%) is very high, after treatment with concentrated acid, XZr-S1 presents a very low content of zirconium (0.3 wt%). Due to the higher microporosity of the Norit based samples, NZr-S1 was able to retain in its structure a higher amount of SZr compared to sample XZr-S1 (Table 3). Complementarily, the surface composition of the Norit based samples was also analyzed by XPS (Table 2 and Figure 2). And it was confirmed the higher loadings of zirconium for samples

NZr and NZr-S2. NZr-S1 sample presented a considerable lower amount of Zr, which means that the treatment of NZr with diluted H<sub>2</sub>SO<sub>4</sub> solution is the most efficient method to maximize sulfated Zr over the carbon surface. The use of concentrated acid promoted the leaching of the Zr, thus remaining only a small amount, probably located inside the pores. Similar results were observed for the xerogel type carbons. The samples with higher pores volumes retained higher amounts of zirconium. In fact, XPS analysis was unable to detect any zirconium in the surface of sample XZr-S1 (Table 3), confirming that the remaining zirconium after H<sub>2</sub>SO<sub>4</sub> treatment is located inside the pores. The XPS analysis of XZr-S2 xerogel sample did not detect as much Zr as seen by WDXRF, probably due to sample heterogeneity. However, values determined by ICP were closer to the ones detected by XPS.

**Figure 2.** XPS spectra of Zr 3d (left) and S 2p (right) binding for the NZr and NZr-S catalysts.

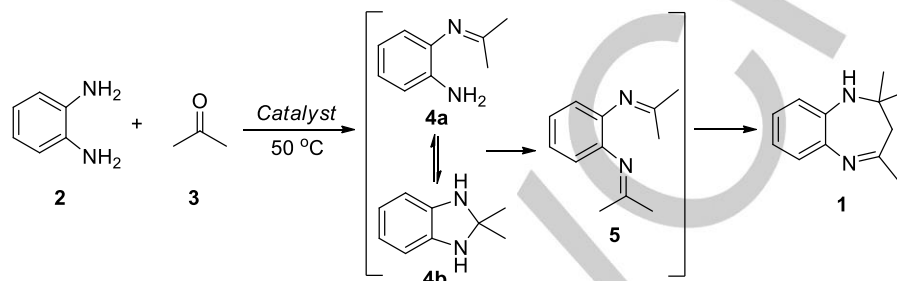
The presence of S and O was also detected for samples NZr-S1 and NZr-S2, although in different %. Obviously, the samples containing Zr showed higher O% due to the presence of ZrO<sub>2</sub> over the carbon surface but also to the oxygenated functional groups generated by the acid treatment (Table 2). Surface analyses of Zr3d and S2p over the catalysts are shown in Figure 2. XPS spectra for the N-Zr and NZr-S samples showed the presence of the typical doublet with binding energies (BE) of 183.68 (Zr3d<sub>5/2</sub>) and 185.7 eV (3d<sub>3/2</sub>) indicating the presence of Zr, also observed for NZr-S1 although at lower BE probably because of small amount of Zr supported over the carbon surface. XPS spectra of S2p binding of NZr-S1 and NZr-S2 samples demonstrated the presence of sulfur. Small differences in BE values were observed which could be attributed to the presence of sulfate groups in Zirconia for NZr-S2 sample and of –SO<sub>3</sub>H functions anchored on the carbon surface for NZr-S1 catalyst.

All these results are in good agreement with the textural properties of these materials which are strongly affected by the presence of Zr. It is important to note that samples NZr and NZr-S2 present similar textural properties. For the xerogel carbon, the sample XZrS1 almost recovered the surface area of the parent carbon.

**Table 3.** Composition (expressed on wt%) of the Zr-supported xerogel carbon materials.

Sample	C 1s <sup>[a]</sup>	O 1s <sup>[a]</sup>	Zr 3d <sup>[a]</sup>	C <sup>[b]</sup>	H <sup>[b]</sup>	N <sup>[b]</sup>	S <sup>[b]</sup>	O <sup>[b]</sup>	Zr <sup>[c]</sup>	S <sup>[c]</sup>	Zr <sup>[d]</sup>
XZr-S1	89.10	10.90	n.d.	86.47	1.65	0.09	0.19	11.79	0.90	0.01	0.33
XZr-S2	80.40	13.64	5.97	62.17	1.27	0.12	0.81	35.63	39.72	1.08	7.60

Determined by [a] XPS [b] elemental analysis [c] WDXRF [d] ICP; n.d. – not detected

**Scheme 1.** Synthesis of benzodiazepine **1** from *o*-phenylenediamine **2** and acetone **3** at 50 °C.

The samples were also characterized by XRD (Figure 3). The XRD patterns confirmed the low crystallinity of ZrO<sub>2</sub> when compared to SZr. Sample SZr was submitted to thermal treatment and its mainly composed by tetragonal SZr. The amorphous ZrO<sub>2</sub> was also observed in XZr-S2 sample whereas XZr-S1 showed the absence of diffraction lines corresponding to Zr. These results are in good agreement with those above mentioned.

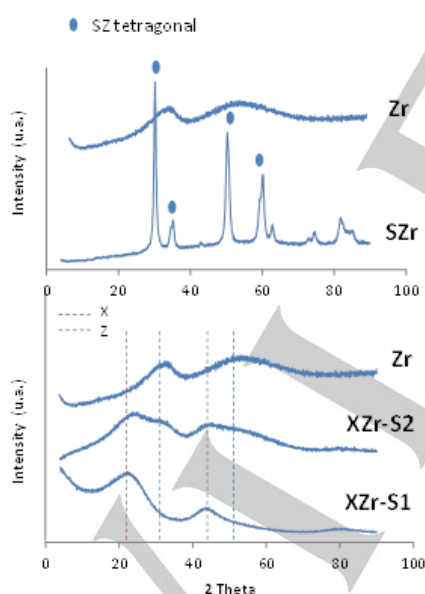
**Figure 3.** XRD patterns for Zr, SZr, XZr-S1 and XZr-S2 samples.

Figure 4 presents the SEM images of SZr supported in carbons. The two carbons present a clear difference in morphology. The

Norit carbon has a more sponge like appearance with clear surface porosity, while the xerogel carbon appears as cleaner surface with sharp edges. The SEM images of the samples with higher amount of Zr (XZr-S2 and NZr-S2) clearly show a heterogeneous distribution of the Zr, indicating that these catalysts are in fact a composite of carbon and zirconia. The excess amount of zirconium source used in the synthesis allowed not only the introduction of ZrO<sub>2</sub> inside the pores, but also its precipitation on the external surface and in the surroundings of the carbon. Several EDS scans in different areas of the sample, confirmed the presence of carbon and of Zr throughout the samples. Even in samples NZr-S1 and XZr-S1 with lower amount of Zr, the EDS analysis over a carbon particle detected the presence of zirconium confirming the incorporation inside the material (complementary material, fig 1). The treatment with concentrated H<sub>2</sub>SO<sub>4</sub> removed all the outer Zr species of the sample, leaving only a small amount of SZr inside the pores of the carbon, as detected by EDS. These results are in agreement with the drastic changes observed in the textural properties and composition of the different carbons.

Figure 5 shows NH<sub>3</sub>-TPD profiles of NZr and NZr-S2 samples. Since the treatment of the catalyst NZr with sulfuric acid can also modify the support, the NH<sub>3</sub>-TPD profile of the carbon support when treated with sulfuric acid is also presented, N-S.

The results evidence the presence of different strength acid sites in the catalysts due to the modifications performed. The carbon support only presents weaker acid sites (dash line) responsible for the peaks at lower temperature, up to 350 °C. The presence of zirconium oxide corresponded to an intensification of groups of medium strength (marked with \*). The catalysts NZr-S2 presents new stronger acid sites (500-650 °C) as a result of the sulfated zirconia.

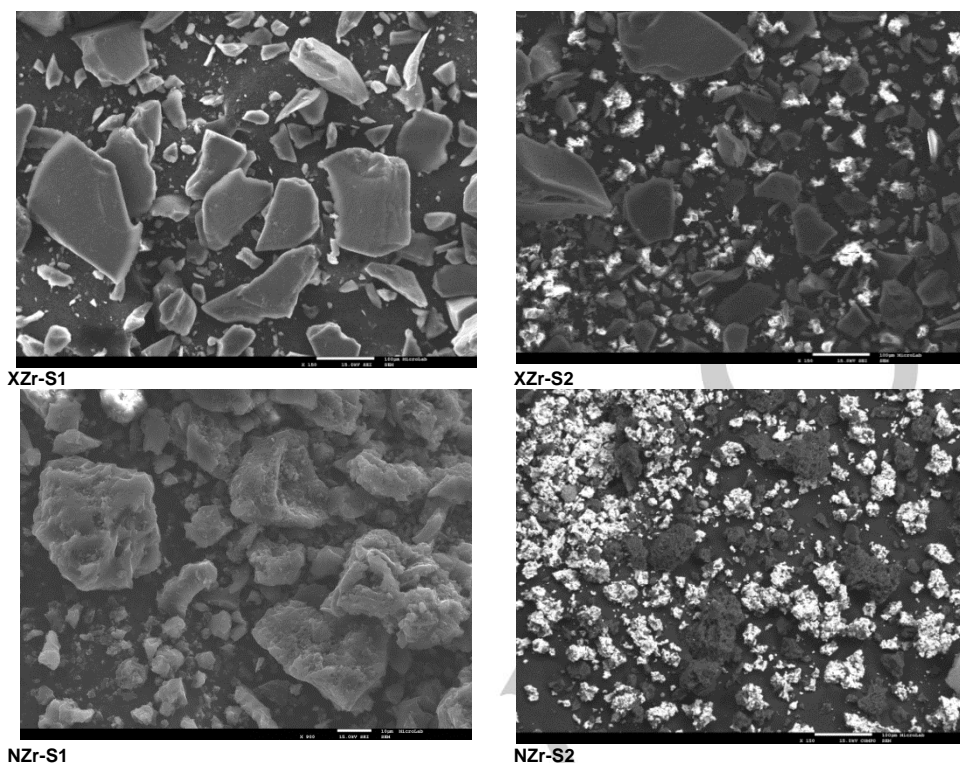


Figure 4. SEM Images of samples NZr-S1, NZr-S2, XZr-S1 and XZr-S2

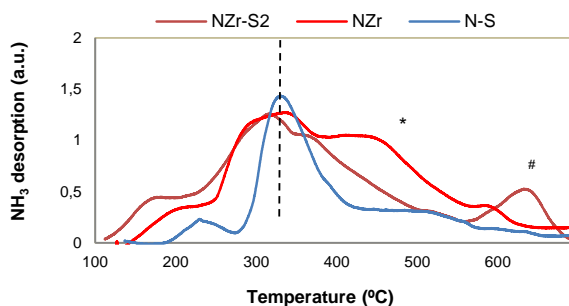


Figure 5.  $\text{NH}_3$ -TPD profiles of Norit carbon catalysts.

Table 4 summarises the amount obtained for the different strength acid sites by deconvolution of the TPD profiles.

Table 4. Deconvolution peaks of  $\text{NH}_3$ -TPD profiles

Sample	mmol $\text{NH}_3$ adsorbed / g $\text{Cat}$			
	150-250 °C	250-350 °C	350-500 °C	500-650 °C
N-S	0.028	0.257	0.327	-
NZr	0.102	0.348	0.238	0.133
NZr-S2	0.027	0.094	0.864	0.519

**Catalytic performance.** The catalysts were tested in the synthesis of benzodiazepines **1** from *o*-phenyldiamine **2** and acetone **3** at 50 °C (Scheme 1). Initially, the reaction was carried out in the presence of non-supported Zr and SZr, as already reported by Reddy and col.<sup>[21, 24]</sup> The authors prepared, isolated and purified by column chromatography on silica gel several benzodiazepines from *o*-phenyldiamine **2** and different substituted ketones, under ambient conditions.

However, we surprisingly observed some interesting findings (Figure 6). The reaction in the presence of both Zr and SZr catalysts, at 50 °C, using similar catalyst amount than that supported on carbon surface, produced high conversion values after only 15 min of reaction time (up to 70%). An analysis of the  $^1\text{H}$  NMR spectra of the crude, when the reaction was achieved in the presence of Zr, demonstrated the almost exclusive presence of a new product whose structure was assigned to compound **4b** by the presence of two signals in the aromatic region, at  $\delta$  6.41 and 6.24 ppm as multiplets, and a singlet at 1.49 ppm corresponding to methyl groups. Interestingly intermediate compound **4a** was not detected.<sup>[20]</sup>

Remarkably, only after 120 min of reaction time, the formation of the benzodiazepine **1** in almost 3% of yield was observed. This intermediate compound was also observed when the reaction was carried out in the presence of SZr. The selectivity to compound **1** increased with the reaction time. These results strongly suggest that the first step of the reaction consisting of imination reaction between reagents followed by formation of compound **4b**, is mainly catalyzed by Lewis acid sites. Whereas the second imination and subsequent electrocyclization are probably promoted by Brønsted acid sites functions that can also be present in the SZr sample.<sup>[25]</sup>

On the other hand, we also investigated the catalytic behavior of the commercial sample Norit-RX3, leading to 55% of conversion with increased selectivity values to **1** (85%) after 1h of reaction time.

Having these results in mind, the authors think that the combination of porous structure of the different carbon supports together with the high acid character of SZr, could make these

solids interesting catalysts for the green synthesis of 2,3-dihydro-1*H*-1,5-benzodiazepines. Although SZr has been extensively used in different organic transformations, as far as we know, only a few examples of carbon supported Zr and SZr have been recently reported.<sup>[26-28]</sup> Among them Zr-supported on carbon nanotubes has been reported for the ketonization of acetic acid.<sup>[29]</sup> In this sense, we tested the carbon supported Zr and SZr in the reaction under study. As can be observed from Figure 7, conversion values of **2** were up to 80%, after the first 15 min of reaction time, when operating in the presence of the N catalysts.

These results are particularly relevant if analyzing the selectivities to benzodiazepine **1**. It was observed that the best selectivities to **1** were obtained in the presence of NZr-S1 and NZr-S2 samples, as expected. The presence of Zr, -SO<sub>3</sub>H functions and carbon support, all of them probably involved in the catalytic reaction, improved significantly the selectivity to **1**.

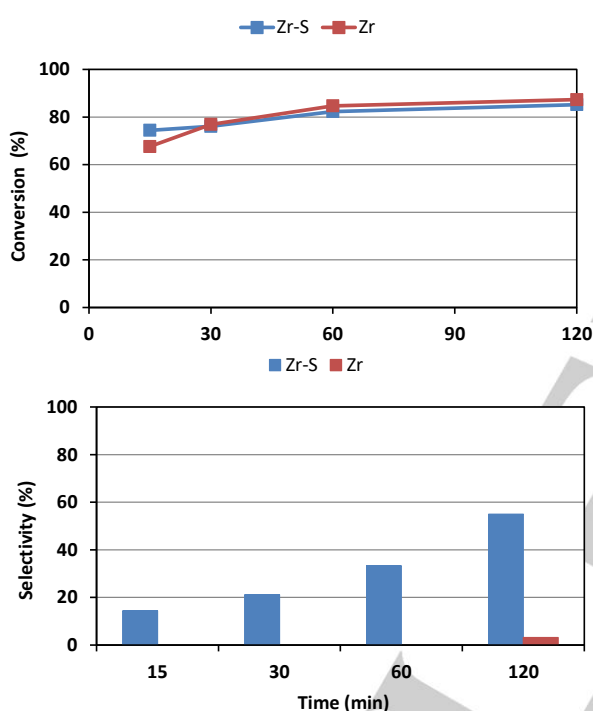


**Figure 6.** Synthesis of benzodiazepine **1** from *o*-phenylenediamine **2** and acetone **3**, at 50 °C, catalysed by Zr or SZr.

Thus, the benzodiazepine **1** was obtained with 80% of selectivity in only 30 min of reaction time in the presence of NZr-S1 catalyst. Whereas the reaction catalyzed by NZr-S2 sample led to compound **1**, with selectivity slightly lower. It is important to note that the benzodiazepine **1** was obtained in almost quantitative yields in the presence of both catalysts after 2 or 3h of reaction time.

The selectivity and activity differences of the catalysts can thus be attributed to their different chemical composition and textural properties. NZr-S1 sample showed lower Zr and S contents but also comprising higher carbon porous surface, whereas NZr-S2 consists of higher Zr and S loadings (Table 2).

These results strongly suggest that there is an optimum concentration of SZr able to efficiently catalyze the reaction

allowing the involvement of the carbon in the process. On the other side, the NZr-S1 catalyst is mainly a microporous sample exhibiting high surface area, in contrast to NZr-S2 sample showing lower  $V_{\text{micro}}$  and higher  $V_{\text{macro}}$ , both parameters influencing the reaction selectivity.

Remarkably the formation of benzodiazepine **1**, with selectivities up to 40% (15 min) becoming 80 and almost 90%, during prolonged reaction times, even in the presence of NZr was observed. This suggests that the Bronsted acid sites present in the carbon surface are the ones involved in the second step of the reaction. This result is especially relevant since allows the eco-friendly synthesis of benzodiazepines avoiding the use of H<sub>2</sub>SO<sub>4</sub>.

Therefore, since these SZr-supported catalysts contain two or more catalytic active sites involved in cascade reactions, the carbon materials herein reported can be considered as bifunctional or multifunctional carbon-based catalysts able to efficiently catalyze the synthesis of benzodiazepines.

In order to explore the influence of the textural properties of the catalysts in the reaction, we also investigated the catalytic behavior of the analogous catalysts based on commercial carbon xerogel. In Figure 7, it is shown the conversion values of reagent **2** in the presence of XZr, and also XZr-S1 and XZr-S2. The conversion values decreased from XZr to XZr-S2 while the selectivity to product **1** follows the inverse trend.

Comparing N and X samples, conversion and selectivity values were maintained in the presence of both supported Zr samples. However, when using carbon supported Zr and SZr catalysts the composition and porosity notably affected the catalytic performance. In the case of using NZr-S catalysts, the oxygenated functions over the carbon surface and the highest  $V_{\text{micro}}$  and  $S_{\text{BET}}$  in NZr-S1 favored the reaction and increased the selectivity to product **1**, probably due to a confinement effect. In contrast, among XZr-S samples, XZr-S2 catalyst with higher loading of SZr exhibited lower conversion values but the best selectivity to **1**, probably due to lower porosity in comparison with XZr-S1 sample.

Additionally, in order to explore the stability of the catalysts in the reaction medium, the reaction under study was carried out in the presence of XZr-S1 which was subsequently removed from the reaction mixture after 15 min of reaction time. It was observed that total conversion values vs time were maintained in comparison to those for reaction in the presence of XZr-S1 catalyst. However, selectivity to benzodiazepine **1** decreased whereas selectivity to **4b** increased from 43 to 60 % after 2h of reaction time, traces of intermediate compounds **4a** and **5** were also detected (Scheme 1). These results strongly suggest that no leaching of the catalytic species occurred and the observed reactivity can be attributed to the reaction in absence of any catalyst. It is noteworthy that the blank experiment under the same experimental conditions gave 34% of total conversion and selectivity to **1** of 5%, during 2h of reaction time.

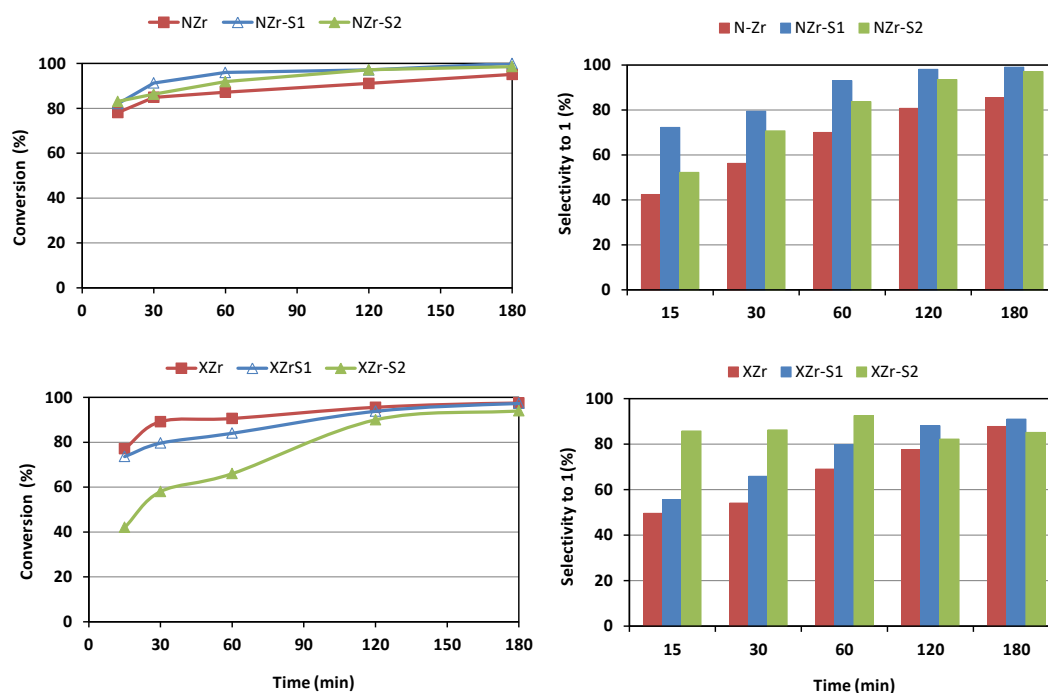


**Figure 7.** Synthesis of benzodiazepine **1** from *o*-phenyldiamine **2** and acetone **3**, at 50 °C, catalyzed by Zr or SZr-supported carbons.

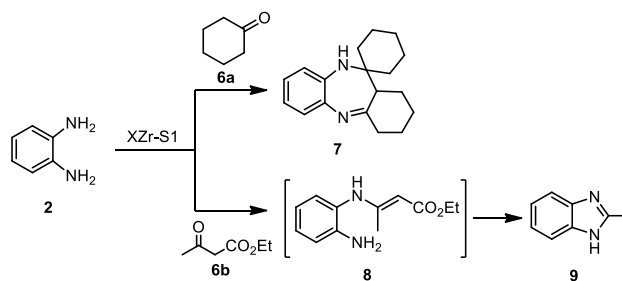
**Table 5.** Catalytic performance of the previously reported catalysts in the synthesis of benzodiazepine **1**

Catalyst	Reaction conditions <sup>[a]</sup>	Time (h)	Conversion (%)	Ref.
HY	1 mmol / 2 mmol / 100 mg, 323 K	2	42	14
		4	93	
Al-MCM-41		6	69	14
Cu(BDC)		6	48	14
Bentonite	2 mmol / 56 mmol / 100 mg, 329 K	1	40	18
		3	60	
K-10 Mont	1.0 mmol / 2.5 mmol / 300 mg, rt	6	89	19a
Zn <sup>2+</sup> -Mont	1.0 mmol / 2.2 mmol / 50mg, rt	5	77	19b
H-MCM-42	1 mmol / 2.5 mmol in acetonitrile / 100 mg, rt	1	87	15
HClO <sub>4</sub> -SiO <sub>2</sub>	1 mmol / 2.5 mmol / 50 mg, rt	1	92	17
SO <sub>4</sub> <sup>2-</sup> /ZrO <sub>2</sub>	No details, rt	2-3	97	21
NZr-S1	1mmol / 10 mmol / 100mg, 323 K	1 (30 min)	96 (93, S=80)	This work

[a] *o*-Phenyldiamine / acetone / Catalyst. S = selectivity.

Table 5 shows some heterogeneous catalysts, reaction conditions and catalytic performances reported in the literature for the synthesis of benzodiazepine **1**. It can be observed that when using the methodology described in this work it is possible to obtain a conversion value of 93% with high selectivity to benzodiazepine **1**, in only 30 min of reaction time, under solvent-free conditions.

Finally, the reaction was explored using other different carbonyl components such as cyclohexanone **6a** and ethyl acetoacetate **6b** in the presence of XZr-S1 (Scheme 2).



**Scheme 2.** Synthesis of benzodiazepine **7** from *o*-phenyldiamine **2** and other carbonyl compounds **6** catalyzed by XZrS1, at 50 °C, under solvent-free conditions.

Thus, when using **6a** it was observed the exclusive formation of the corresponding benzodiazepine **7** in 76%, after 3h of reaction time, as unique reaction product, and in good agreement with data previously reported using other catalytic systems (Figure 8)<sup>[14]</sup>; in this case, the lower conversion values are attributed to the steric hindrance of the corresponding carbonyl compound regarding to acetone **3**. On the other hand, the reaction in the presence of ethyl acetoacetate **6b** led to the total transformation of *o*-phenyldiamine **2** yielding a mixture of the intermediate **8**,

resulting of the imination reaction between reagents and subsequent tautomerization, and of

2-methylbenzimidazole **9** (compounds **8/9** ratio = 77:23 after 15 min of reaction time), instead of the corresponding benzodiazepine. At this regard, Figure 8 depicts the evolution of the reaction in which compound **8** is transformed into **9**. These results are in accordance with those previously reported where the authors described the synthesis of 2-methylbenzimidazole from *o*-phenyldiamine **2** and ethyl acetoacetate **6b** upon microwave irradiation in water<sup>[30]</sup> or promoted by ammonium salts at 85 °C.<sup>[31]</sup>

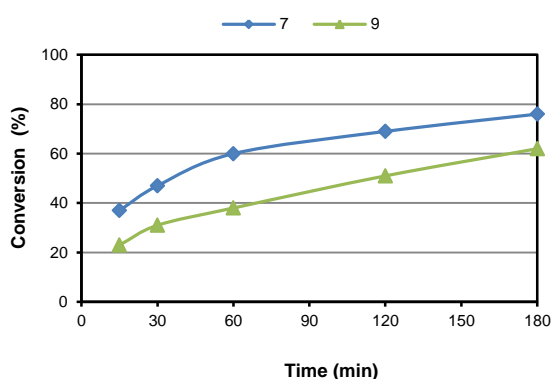


**Figure 8.** Synthesis of benzodiazepine **7** from *o*-phenyldiamine (**2**) and cyclohexanone (**6a**) (blue) and 2-methylbenzimidazole (**9**) from *o*-phenyldiamine (**2**) and ethyl acetoacetate (**6b**) (green) catalyzed by XZrS1, at 50 °C, under solvent-free conditions.

## Conclusions

This work reports for the first time a new series of promising porous catalytic carbon materials, functionalized with Lewis and Brønsted acid centers, useful in the green synthesis of 2,3-dihydro-1*H*-1,5-benzodiazepine from *o*-phenyldiamine and ketones. Although SZr has been widely used in interesting organic transformations, only a few examples of carbon supported Zr and SZr have been recently reported. NZr, XZr and the corresponding sulfated catalysts led to high conversions and selectivity values to compound **1** in comparison with non-supported Zr and SZr.

Remarkably, our results demonstrated that while the non-supported Zr sample catalyzes the first steps of the reaction, comprising the monoimination reaction between reagents and subsequent intramolecular cyclization, leading to the 2,3-dihydrobenzimidazole **4b**, the Brønsted acid sites in the non-supported SZr promote the second imination and electrocyclization reactions resulting in benzodiazepine **1**. However, the investigated reaction in the presence of Zr or SZr-supported on carbon catalysts yielded the compound benzodiazepine **1** with increased selectivity even at short reaction times.

An especially relevant result is the formation of product **1**, with good conversions and selectivity, in the presence of the supported catalysts, NZr and XZr, avoiding the use of H<sub>2</sub>SO<sub>4</sub>

solutions. It is also confirmed the involvement of the carbon support in the reaction under study. In this sense, the combination of porous structure of carbon supports together with the acid character of supported Zr or SZr allows a much more sustainable synthesis of benzodiazepine **1**, affording high activity and selectivity while using an environmentally friendly catalyst. These new catalysts are even much more efficient than zeolites or mesoporous silica catalysts<sup>[9]</sup>.

One of the most relevant results is the high catalytic performance of carbons with low Zr loading, confirming the combination of material properties between carbon and Zr.

In summary, the Zr and SZr-supported carbon catalysts herein reported were found to be multifunctional carbon-based catalysts involved in the synthesis of benzodiazepines. The observed reactivity opens the doors to explore other interesting cascade reactions for the synthesis of relevant heterocyclic systems.

## Experimental Section

The selected carbon materials were two commercial carbons, i) Norit RX3 (NORIT Nederland B.V.) and ii) mesoporous carbon (Xerolutions S.L.). All reagents and solvents were purchased from Sigma-Aldrich.

### 1. Synthesis of catalysts

**1.1. Synthesis of Zr and SZr.** A solution of ZrCl<sub>4</sub> (1 g) in of water (10 mL) was treated with ammonia until pH = 10. The solid was then filtered, washed with abundant water and dried at 110 °C. SZr was prepared from Zr (1 g) and H<sub>2</sub>SO<sub>4</sub> 0.5M (15 mL) and the mixture was stirred, at room temperature, during 30 min. The solid was filtered, washed with abundant water and calcined at 600 °C during 4 h.

**1.2. Synthesis of Zr-supported carbons.** To a solution of ZrCl<sub>4</sub> (1 g) in water (100 mL) the corresponding carbon material (1 g) was added and the reaction mixture was stirred during 1 h. Subsequently the suspension was treated with ammonia until pH = 10 and stirred during 1h. The solid was then filtered, washed with abundant water and dried at 110 °C.

**1.3. Synthesis of SZr-supported carbons. Method A:** A suspension of the corresponding Zr-supported carbon was treated with commercial H<sub>2</sub>SO<sub>4</sub> (98%) (15 mL)<sup>[32]</sup> and the reaction mixture was stirred during 90 min. The solid was then filtered, washed with abundant water and dried at 110 °C during 12h. **Method B:** A suspension of the corresponding Zr-supported carbon was treated with H<sub>2</sub>SO<sub>4</sub> 0.5 M (15 mL) and the reaction mixture was stirred during 30 min. The solid was then filtered, washed with abundant water and dried at 110 °C during 12h.

Then, two different series of carbon materials were prepared: i) NZr, NZr-S1 and NZr-S2; ii) XZr, XZr-S1 and XZr-S2 where N = Norit-RX3, X = xerogel, Zr = ZrO<sub>2</sub>, Zr-S1 = SO<sub>4</sub><sup>2-</sup>/ZrO<sub>2</sub> synthesized by using the method A and Zr-S2 = SO<sub>4</sub><sup>2-</sup>/ZrO<sub>2</sub> synthesized by using the method B.

**2. Characterization of the catalysts.** The materials under study were characterized by: a) N<sub>2</sub> adsorption-desorption isotherms at 77K

(Quantachrome Autosorb iQ2-Series); b) Hg porosimetry carried out in a Quantachrome Poremaster 60; c) X-Ray Photoelectron Spectra (XPS) registered in a K-Alpha Thermo Scientific Spectroscopy; for the analysis of the XPS peaks, the C1s peak position was set at 284.5 eV and used as reference to locate the other peaks; d) Wavelength Dispersive X-Ray Fluorescence analysis (WDXRF) performed in a Bruker S8Tiger; e) Elemental analysis (C, H, N and S) performed in a LECO CHNS-932 instrument; f) thermogravimetry in a thermobalance Setaram SETSYS Evolution; g) Inductively coupled plasma atomic emission spectroscopy (ICP-AES) to determine the bulk concentration of Zr; h) Scanning Electron Microscopy (SEM) images obtained in a Hitachi S2400 analytical SEM with a Bruker energy dispersive spectroscopy (EDS) detector for elemental analysis. The surface acid groups were probed by temperature-programmed desorption of ammonia (NH<sub>3</sub>-TPD) technique. Prior to NH<sub>3</sub>-TPD, the catalyst was pre-treated at 200°C under helium atmosphere for 1 hour. The temperature was then decrease to 125 °C and the sample was saturated under a flow of NH<sub>3</sub> in He for 1 h. The physisorbed ammonia was removed by flushing with He for 1 h. The temperature programmed desorption of ammonia (NH<sub>3</sub>-TPD) experiments were performed from 125 °C to 700 °C, remaining 15 min at the highest temperature.

**3. Catalytic performance.** In a typical experiment, a mixture of *o*-phenylenediamine **2** (1 mmol) and acetone **3** (10 mmol) in a three-necked vessel, equipped with thermometer, was placed on a multiexperiment work station StarFish (Radley's Discovery Technologies IUK). When the temperature reaches 50 °C, the catalyst was added (100 mg) and the reaction mixture was maintained during 240 min. The samples were periodically taken at 15, 30, 60, 120, 180 and 240 min, diluted with ethyl acetate (0.5 mL), and the catalyst was filtered off and the solvent evaporated *in vacuo*. The reaction were followed by TLC chromatography performed on DC-Aulofolien/Kieselgel 60 F245 (Merk) using mixtures of CH<sub>2</sub>Cl<sub>2</sub>/EtOH 98:2 as eluent.

The reaction products were characterized by <sup>1</sup>H NMR spectroscopy. NMR spectra were recorded by using a Bruker AVANCE DPX-300 spectrometer (300 MHz for <sup>1</sup>H). <sup>1</sup>H chemical shifts in [D<sub>6</sub>]DMSO are referenced to internal tetramethylsilane. Characterization data of benzodiazepines **1** and **7** [14] and 2-methyl benzoimidazole **9** are in good agreement with those previously reported using other catalytic systems. [29, 30]

## Acknowledgements

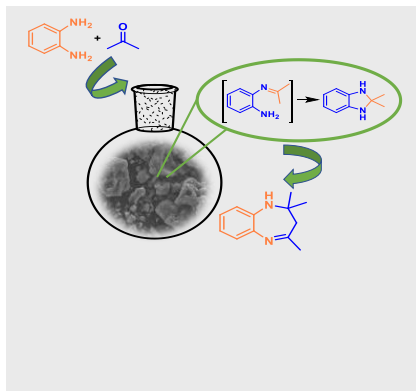
This work has been supported by Spanish Ministry (CTM 2014-56668-R project) and Junta de Extremadura (IB16167). This work was supported by the Associate Laboratory for Green Chemistry- LAQV which is financed by national funds from FCT/MCTES (UID/QUI/50006/2013) and co-financed by the ERDF under the PT2020 Partnership Agreement (POCI-01-0145-FEDER - 007265). Ines Matos thanks FCT for the Investigador FCT contract IF/01242/2014/CP1224/CT0008 and M. Bernardo for post-doc fellowship (SFRH/BPD/93407/2013), Carlos J. Durán-Valle also thanks the Junta de Extremadura for the grant to make a stay at the UNL (MOV15B004).

**Keywords:** zirconia and sulphated zirconia carbon catalysts • multifunctional carbon catalysts • cascade reactions • benzodiazepines

- [1] P. Serp, J.L. Figueiredo, Carbon Materials for Catalysis, John Wiley & Sons, Hoboken, NJ, 2009.
- [2] J. López-Sanz, E. Pérez-Mayoral, E. Soriano, D. Omenat-Morán, C. J. Durán, R. M. Martín-Aranda, I. Matos, I. Fonseca, *ChemCatChem* **2013**, *5*, 3736–3742.
- [3] M. Godino-Ojer, A. J. López Peinado, R. M. Martín Aranda, J. Przepiorski, E. Pérez-Mayoral, E. Soriano, *ChemCatChem* **2014**, *6*, 3440–3447.
- [4] M. Godino-Ojer, E. Soriano, V. Calvino-Casilda, F. J. Maldonado-Hódar, E. Pérez Mayoral, *Chem. Eng. J.* **2017**, *314*, 488–497.
- [5] E. Pérez-Mayoral, V. Calvino-Casilda, E. Soriano, *Catal. Sci. Technol.* **2016**, *6*, 1265–1291.
- [6] M. Godino-Ojer, A. J. López-Peinado, F. J. Maldonado-Hódar, and E. Pérez-Mayoral, *ChemCatChem* **2017**, *9*, 1422–1428.
- [7] M. Godino-Ojer, R. M. Martín-Aranda, F. J. Maldonado-Hódar, A. F. Pérez-Cadenas, E. Pérez-Mayoral, *Mol. Catal.* **2018**, *445*, 223–231.
- [8] J. Macht, R. T. Carr, E. Iglesia, *J. Catal.* **2009**, *264*, 54–88.
- [9] D. Fraenkel, N. R. Jentzsch, C. A. Starr, P. V. Nikrad, *J. Catal.* **2010**, *274*, 29–51.
- [10] K. Arata, *Green Chem.* **2009**, *11*, 1719–1728.
- [11] G. D. Yadav, J. J. Nair, *Micropor. Mesopor. Mat.* **1999**, *33*, 1–48.
- [12] J. B. Bariwal, K. D. Upadhyay, A. T. Manvar, J. C. Trivedi, J. S. Singh, K. S. Jain, A. K. Shah, *Eur. J. Med. Chem.* **2008**, *43*, 2279–2290.
- [13] R. K. Singha, S. Sharma, A. Kaura, M. Sainia, S. Kumar, Iran. J. Catal. **2016**, *6*, 1–21.
- [14] M. Jeganathan, K. Pitchumani, *ACS Sustainable Chem. Eng.* **2014**, *2*, 1169–1176.
- [15] S. A. Majid, W. A. Khanday, R. Tomar, *J Biomed Biotechnol.* **2012**, <http://dx.doi.org/10.1155/2012/510650>
- [16] M. R. Shushizadeh, N. Dalband, *J. Nat. Pharm. Prod.* **2012**, *7*, 61–64.
- [17] H. M. Meshram, P. N. Reddy, P. V. Murthy, J. S. Yadav, *Synth. Commun.* **2007**, *37*, 4117–4122.
- [18] M. Munoz, G. Sathicq, G. Romanelli, S. Hernandez, C.I. Cabello, I.L. Botto, M. Capron, *J. Porous Mater.* **2013**, *20*, 65–73.
- [19] R. Varala, R. Enugala, S. R. Adapa, *Arkivoc* **2006**, *xiii*, 171–177.
- [20] B. González, R. Trujillano, M. A. Vicente, A. Gil, V. N. Panchenko, E. A. Petrova, M. N. Timofeeva, *Appl. Clay Sci.* **2017**, *146*, 388–396.
- [21] V. M. Reddy, P. M. Sreekanth, *Tetrahedron Lett.* **2003**, *44*, 4447–4449.
- [22] M.S. Scurrall, *Appl. Catal.* **1987**, *34*, 109–117.
- [23] K. Saravanan, B. Tyagi, H. C. Bajaj, *Appl. Catal. B: Env.* **2016**, *192*, 161–170.
- [24] B. M. Reddy, P. M. Sreekanth, P. Lakshmanan, *J. Mol. Catal. A: Chem.* **2005**, *237*, 93–100.
- [25] N. Katada, J.I. Endo, K.I. Notsu, N. Yasunobu, N. Naito, M. Niwa, *J. Phys. Chem. B.* **2000**, *104*, 10321–10328.
- [26] P. Dhanasekaran, S. R. Williams, D. Kalpana, S. D. Bhat, *RSC Adv.* **2018**, *8*, 472–480.
- [27] P. Madkikar, X. Wang, T. Mittermeier, A. H. A. M. Videla, C. Denk, S. Specchia, H. A. Gasteiger, M. Piana, *J. Nanostruct. Chem.* **2017**, *7*, 133–147.
- [28] C. Liu, L. D. Pfefferle, G. L. Haller, *Top. Catal.* **2014**, *57*, 774–784.
- [29] K. Wu, M. Yang, W. Pu, Y. Wu, Y. Shi, H.-sh. Hu, *ACS Sustainable Chem. Eng.* **2017**, *5*, 3509–3516.
- [30] Z.-X. Wang, H.-L. Qin, *J. Heterocyclic Chem.* **2005**, *42*, 1001–1005
- [31] B. C. Raju, N. D. Theja, J. A. Kumar, *Synt. Commun.* **2009**, *39*, 175–188.
- [32] C. J. Durán-Valle, M. Madrigal-Martínez, M. Martínez-Gallego, I. M. Fonseca, I. Matos, A. M. Botelho do Rego, *Catal. Today* **2012**, *187*, 108–114.

## FULL PAPER

This work reports a new series of porous catalytic carbon materials, functionalized with Lewis and Brønsted acid centers, active in the green synthesis of 2,3-dihydro-1H-1,5-benzodiazepine. The studies demonstrated that both the carbon porous structure and acid site types are involved in the reaction. The texture and composition of the investigated carbon materials strongly influenced the catalytic performance.



*M. Godino-Ojer, L. Milla-Diez, I. Matos, C. J. Durán-Valle, M. Bernardo, I. M. Fonseca\* and E. Pérez Mayoral\**

**Page No. – Page No.**  
**Enhanced catalytic properties of carbons supported zirconia (Zr) and sulfated zirconia (SZr) in the green synthesis of benzodiazepines**